Interaction of the Solar Wind

with the Moon

Antonio Alfonso-Faus and P. J. Kellogg

COSMIC RAY GROUP

School of Physics and Astronomy

UNIVERSITY OF MINNESOTA

5/1/97

Interaction of the Solar Wind

with the Moon

Antonio Alfonso-Faus and P. J. Kellogg

School of Physics and Astronomy
University of Minnesota
Minneapolis, Minnesota

NSG - 281 - 62

CR-117
June, 1968

Interaction of the Solar Wind with the Moon[*]

by

Antonio Alfonso-Faus and P. J. Kellogg

Abstract

The problem of the interaction of the solar wind with the moon is attacked from a kinetic-theory point of view. The boundary conditions are the total absorption of the solar-wind particles by the moon's surface and the magnetic transparency of the lunar body; these conditions imply the absence of an up-stream shock wave.

The analytical treatment of the ion component gives the gross features of the structure of the interaction. The main feature is the presence of an empty cavity of conical shape, that has the length of a few tens of moon radii and is approximately given by the ratio of the solar wind velocity and the product of the ion thermal velocity times the sine of the angle between the interplanetary magnetic field and the velocity of the solar wind. This angle does not strongly affect the orientation of the cavity which is parallel to the solar wind velocity relative to the moon's frame. The disturbance in plasma density and flux occurs almost entirely inside the cylinder tangential to the moon and parallel to the bulk velocity of the plasma. This cavity has been observed by the satellite Explorer 35.

Two important effects are found due to electron pressure: a) shortening of the length of the wake and b) weakening of the gradients of density across the boundary. The two effects are analyzed separately and an effective temperature for the ions is defined in order to take into account the presence of the electrons.

The drop in density across the boundary of the cavity produces a system of currents that increases the magnetic field strength inside the cavity. The problem is idealized by considering that the drop occurs within a Larmor distance; in this way one arrives at a situation similar to the problem of a solenoid. The present observations show the increase in the magnetic field strength inside the cavity. They also show a decrease across the boundary and an increase just outside the cavity; further refinements to the theory may explain these observations, or they may be the result of a contribution from a weak magnetic field, intrinsic to the moon, that has been distorted by the solar wind.

1. Introduction

The purpose of this work is a theoretical treatment of the interaction of the solar wind with the moon. Either no intrinsic magnetic field, or a very low one, is present in the moon (Sonett et al., 1967; Ness et al., 1967). Hence, the solar-wind particles are free to directly hit the surface, and we will consider that these particles are absorbed and/or neutralized, so that they become disconnected from the plasma.

Since the solar wind is a magnetized plasma, the average electrical conductivity of the moon is also decisive in determining the nature of the interaction. Gold (1966) considered the conductivity high enough to have a piling up of magnetic field lines, and the subsequent formation of a lunar magnetosphere and shock wave. We take the opposite case of low electrical conductivity, or complete transparency of the moon to the magnetic field, as the experimental results from Explorer 35 indicate (Ness et al., 1967).

The solar wind is composed mainly of protons and electrons that arrive at 1 a.u. with a bulk velocity, more or less radially from the sun, which is much higher than the ion thermal speed and much lower than the electron thermal speed. We will take full advantage of these properties that give the order of importance of the different mechanisms at play. We shall first consider the ions alone, since they carry most of the inertia of the stream, and we will use the guiding-center approach. Recently, Whang (1967), has presented a numerical solution based upon similar considerations; the results from our analytical expressions are in complete agreement with this author's work.

After this, we include the electron component and its interaction with the ions. We prove that this effect is of the same order of magnitude as the ion-pressure effect, as far as the closing of the wake is concerned. Furthermore, the gradient of ion density across the boundary is strongly affected by the presence of the electron component. Finally, we analyze the effect of the surface currents and the resultant distortion of the magnetic field. Recently Whang (1968) has considered the same problem; again, there is agreement between his numerical solution and our results.

Michel (1967 and 1968) presents a hydrodynamic analog as a solution to the problem, ignoring the detailed structure of the plasma. We take a kinetic-theory approach that allows us to treat what is present in the solar wind: ions, electrons, electric and magnetic fields.

2. Cold Plasma Approximation

Our first approach is to neglect the ion thermal motions. Under this simplification, the streaming magnetized plasma is composed of a parallel stream of cold ions embedded in a cloud of thermal electrons.

Since the moon is considered here as a perfect absorber, its presence produces an empty space in the stream; reversing the motion, i.e. considering the plasma at rest and the moon moving through it at the solar wind velocity, the moon is sweeping the ions and electrons and therefore leaving a cylindrical empty cavity that is parallel to its velocity. Since the electrons are thermal, they tend to get inside the empty cavity and, at the same time, they are held back by the ion's attraction that preserves the quasi-neutrality of the plasma; the ions are under this electron pressure that reduces the size of the cylindrical cavity, i.e. it is modified to a conical shape. Due to this effect,

the straight line path of the ions will get slightly curved towards

the interior of the cylinder. The thermal electrons, trying to get inside

the empty cylinder, will produce some charge separation which in turn

will be the source of the electric fields that hold them back.

3. Ion Distribution

In order to get the ion distribution function we use the following

assumptions:

a) Far from the moon the distribution function is Maxwellian; this

is then one of the boundary conditions for the solution of Boltzmann's

equation.

b) The surface of the moon acts as a perfect sink for the ions that

happen to strike it; this completes the boundary conditions required to

specify the solution. The assumption implies that, in the vicinity of

the moon, not all the states of the particles in phase-space are present;

a state is missing if the motion of the particle under time reversal

happens to be along a trajectory that intersects the moon's surface.

c) Since the mean free path of the particles in the solar wind is

of the order of 1 a.u. at the earth's orbit, we consider the plasma in a

collisionless state. This makes tractable the problem of finding the

analytical expressions for the trajectory of each particle in the magnetic

plasma.

d) The ions move under the effect of the following forces:

$$\text{gravitational} \qquad \frac{GM_{\mathbb{C}} M}{R_{\mathbb{C}}^2} \simeq 2.6 \times 10^{-22} \text{ dynes}$$

$$\text{electric} \qquad \frac{k\,T}{R_{\mathbb{C}}} \;\simeq\; 8 \times 10^{-20} \text{ dynes}$$

$$\text{magnetic} \qquad \frac{e\,v_{\perp}B_{o}}{c} \;\simeq\; 4 \times 10^{-18} \text{ dynes}$$

where we have used $T = 10^5 \; {}^{o}K$, and $v_{\perp}$ is the component of the thermal velocity perpendicular to the magnetic field lines. It is seen that the magnetic forces dominate the ion motion; hence, the trajectories are spirals along the magnetic field lines.

If the electric potential, which is of the order of some kT/e, varies considerably over distances much shorter than the moon's radius, then the electric forces dominate the ion motion. This is the case for a small region near the back of the moon, as shown later.

From the above assumptions it will be seen that we already have the solution to the collisionless Boltzmann's equation. At a point far from the moon the distribution is Maxwellian. Near the moon the distribution is Maxwellian, except that not all states of the velocity are present. The problem reduces to find these missing states at each particular point.

Figure 1 presents the frame of reference, its origin at the moon's center, x parallel to the magnetic lines, y perpendicular to x in the plane of the magnetic lines and the solar-wind velocity $\overline{V}_{o}$, and z normal to this plane. The velocity $\overline{v}_{p}$ of an arbitrary particle p is given by $\vec{v}_{p} = \vec{V}_{o} + \vec{v}_{\parallel} + \vec{v}_{\perp}$, where $\vec{V}_{o}$ is the solar wind velocity that makes an angle α with the magnetic field lines, $\vec{v}_{\parallel}$ is the projection of the thermal velocity of the ions along the B lines and $\vec{v}_{\perp}$ its projection into a plane perpendicular to the B lines; this projection gives a circling motion whose phase angle is specified by ψ.

Projecting $\vec{v}_p$ along the coordinate axes one gets:

$$v_x = \frac{dx}{dt} = V_o \cos \alpha + v_{//}$$

$$v_y = \frac{dy}{dt} = V_o \sin \alpha + v_{\perp} \sin \psi \tag{1}$$

$$v_z = \frac{dz}{dt} = v_{\perp} \cos \psi$$

Using the explicit time dependence for $\psi = \psi_o + \omega t$ where ω is the ion cyclotron frequency eB_o/Mc, ψ_o the initial phase angle, and noting that V_o, $v_{//}$, $v_{\perp}$, and ψ_o are constant, we integrate the equations in (1) to obtain the trajectory:

$$x = x_o + (V_o \cos \alpha + v_{//}) \, t$$

$$y = y_o + V_o t \sin \alpha - \frac{v_{\perp}}{\omega} [\cos (\psi_o + \omega t) - \cos \psi_o] \tag{2}$$

$$z = z_o + \frac{v_{\perp}}{\omega} [\sin(\psi_o + \omega t) - \sin \psi_o]$$

where x_o, y_o and z_o are the coordinates of the ion at time $t = 0$. A state is missing at the point x_o, y_o, z_o, if the motion of the ion from $t = 0$ to $t = -\infty$ is along a trajectory that intersects the moon's surface; thus, the missing states are given by those values of $v_{//}$, $v_{\perp}$ and ψ_o such that

$$x^2 + y^2 + z^2 = R_{\mathbb{C}}^2 \quad \text{for some } t \leq 0 \tag{3}$$

Since the ion Larmor's radius $L_i = v_{\perp}/\omega$ is much smaller than the moon's radius, we may average out the circling motion of the ions and consider the trajectory of their guiding center. In this way the

system (2) reduces to

$$x = x_o + (V_o \cos \alpha + v_{||}) \, t$$

$$y = y_o + V_o \, t \sin \alpha \tag{4}$$

$$z = z_o$$

From the third expression in (4) it is seen that in the guiding center approach the ion motions are constrained to be in planes z = constant; therefore, the presence of the moon affects only the region between the two parallel planes, perpendicular to the z axes, $z = \pm R_{\mathbb{C}}$. Hence, the three-dimensional problem reduces to a two-dimensional one. Calling $R = (R_{\mathbb{C}}^2 - z_o^2)^{1/2}$, which is the radius of the circle intersected by the plane $z = z_o$ and the lunar sphere, condition (3) is now given by

$$x^2 + y^2 = R^2 \quad \text{for some } t \le 0 \tag{5}$$

where

$$x = x_o + (V_o \cos \alpha + v_{||}) \, t$$

$$y = y_o + V_o \, t \sin \alpha \tag{6}$$

are the equations of the two-dimensional trajectory in the plane $z = z_o$.

From (6) it is seen that the only thermal contribution that comes in is the component $v_{||}$; thus, the missing states are given by a cut in velocity space along the $v_{||}$ axis. The problem reduces to finding the values of $v_{||}$ for which there exist a $t \le 0$ such that $x^2 + y^2 = R^2$. Substituting x and y from (6) into (5) and solving for t one gets:

$$t = \frac{- b \pm (b^2 - 4 \, ac)^{1/2}}{2 \, a} \tag{7}$$

where

$$a = V_o^2 + V_{||}^2 + 2 V_o v_{||} \cos \alpha$$

$$b = 2V_o x_o \cos \alpha + 2V_o y_o \sin \alpha + 2x_o v_{||} \tag{8}$$

$$c = x_o^2 + y_o^2 - R^2$$

The missing states are given by the values of $v_{||}$ such that t is real and ≤ 0, i.e.:

$$b^2 - 4ac > 0 \tag{9}$$

and

$$b \geq 0 \tag{10}$$

since the a that appears in the denominator of (7) is always >0. Hence, the bounds of the forbidden range of $v_{||}$ are given by the roots of the equations:

$$b^2 - 4ac = 0 \tag{11}$$

and

$$b = 0 \tag{12}$$

Solving for $v_{||}$, we get two bounds from (11) and one from (12):

$$V_o \frac{x_o y_o \sin \alpha + (R^2 - y_o^2) \cos \alpha \pm (x_o^2 + y_o^2 - R^2)^{1/2} R \sin \alpha}{y_o^2 - R^2} \tag{12a}$$

$$- V_o \frac{x_o \cos \alpha + y_o \sin \alpha}{x_o} \tag{12b}$$

Since the two conditions (9) and (10) have to be satisfied simultaneously, one has to combine the bounds (12a) and (12b) to get the absolute bounds of $v_{\parallel}$. We call the two roots in (12a) v_1 and v_2 ($v_1 < v_2$), and obtain the following four regions, sketched in Figure 2, that are bounded by the two parallel planes normal to the z axis, $z_o = \pm R_{\mathbb{C}}$:

a) outside the cylinder parallel to $\vec{B}$:

<u>Region I</u>, $y_o < -R_{\mathbb{C}}$, no missing states; the presence of the moon is not felt in this region.

<u>Region II</u>, $y_o > R_{\mathbb{C}}$, missing states given by

$$v_1 < v_{\parallel} < v_2$$

b) inside the cylinder parallel to $\vec{B}$:

<u>Region III</u>, $x_o < 0$, missing states given by

$$- \infty < v_{\parallel} < v_1$$

<u>Region IV</u>, $x_o > 0$, missing states given by

$$v_2 < v_{\parallel} < \infty$$

In the special case $\alpha = 0$, meaning that the magnetic field lines are parallel to the solar wind velocity, one gets from (12a) $v_1 = v_2 = -V_o$ so that region II (Figure 2) has no missing states, an obvious results since by symmetry the regions I and II are identical in this particular case. The disturbed region is confined to the interior of the cylinder, and we get back the wake obtained in the cold plasma approach. In this case the cylindrical wake is modified by electron pressure alone; the thermal motions of the ions do not contribute anything to the cold plasma approach, except for surface currents at the boundary of the wake.

The signs of the relevant bounds are presented in Figure 2. One of the roots (12a) vanishes when crossing the cylindrical wake of the cold plasma approach; for example, along ab and ed $v_1 = 0$, while along bc and fe $v_2 = 0$. By tracing the roots in Figure 2 we can make general statements regarding the geometry of the curves of constant density: referring the density n to the unperturbed density n_o, the straight lines ab and fe are always part of the curve of constant density 0.5; all the curves of density $\leq$ 0.5 are always located inside the cold plasma wake, cylinder acfd, while the exterior of this cylinder contains all the curves of density $\geq$ 0.5. Thus, 50% of the constant density curves are located inside the cold plasma wake. The locus of points at which the two roots (12a) are equal in absolute value but opposite in sign is given by:

$$x \, y \, \tan \alpha - y^2 + R^2 = 0 \qquad (13)$$

which is a hyperbola and corresponds to curve og in Figure 2. Above and below this curve, the average velocity is given by $\vec{V}_o$ plus the contribution from the thermal motions along the magnetic field lines which give an average velocity inclined toward the central part of the wake. The points on og have average velocity exactly equal to $\vec{V}_o$, since the thermal contribution is symmetric there. Since the width of the cuts in velocity space (along the $v_{\parallel}$ axis) is broader than the thermal speeds, the possibility of the two stream instability is there. The growth rate of this instability is of the order of the plasma frequency, i.e. proportional to the square root of the density, and since the density is increasing away from the moon, the growth rate becomes high enough for the instability to exist. This instability would thermalize the particles in the plasma causing it to behave more like a fluid.

4. Length of the Wake

The remarks made in the last section on the density distribution are also valid for the flux distribution, since the thermal velocity of the ions is much smaller than V_o; this means that the curves of constant density are also curves of constant flux, to a good approximation. The remarks are general in the sense that they do not depend on the particular values of the solar wind parameters (density, temperature, velocity and magnetic field strength). To get a quantitative picture of the distribution of densities and fluxes, we need the numerical values along the axis of the wake $y = x \tan \alpha$ which give a measure of its length. In order to do that, we first express the roots (12a) in terms of the coordinates r, λ of figure 7:

$$V_o \frac{- r \lambda \sin \alpha + (R^2 - \lambda^2) \cos \alpha \pm (r^2 + \lambda^2 - R^2)^{1/2} R \sin \alpha}{r^2 \sin^2 \alpha + \lambda^2 \cos^2 \alpha + 2r\lambda \sin \alpha \cos \alpha - R^2} \qquad (14)$$

The density at a particular point is given by the difference between the unperturbed density n_o and the integral of the distribution function over the forbidden interval at that point:

$$\frac{n}{n_o} = 1 - \frac{1}{\pi^{1/2}} \int_{\frac{v_1}{v_{th}}}^{\frac{v_2}{v_{th}}} e^{-x^2} \, dx \qquad (15)$$

$$\text{where } v_{th} = \left(\frac{2 k T_{\parallel}}{M} \right)^{1/2} \qquad (16)$$

In a similar way, the flux is given by the difference between the unperturbed flux $\overline{n_o V_o}$ and the integral of the distribution function, times the velocity of the particle, over the forbidden interval:

$$\overline{nV} = n_o \vec{V}_o - n_o \frac{1}{v_{th}\pi^{1/2}} \int_{v_1}^{v_2} (\vec{V}_o + \vec{v}_{\parallel}) \ e^{-(v_{\parallel}/v_{th})^2} \ dv_{\parallel} \tag{17}$$

$$= n\vec{V}_o - \frac{n_o V_{th}}{2\, \pi^{1/2}} \frac{\vec{B}}{B} \ [e^{-(v_2/v_{th})^2} - e^{-(v_1/v_{th})^2}] \tag{18}$$

Along the axis of the wake, $y = x \tan \alpha$ or $\lambda = 0$, we get the roots v_1 and v_2 from (19)

$$V_o \ \frac{R^2 \cos \alpha \pm (r^2 - R^2)^{1/2} R \sin \alpha}{r^2 \sin^2 \alpha - R^2} \tag{19}$$

and in the case $r \gg R$ we can expand (19) and get:

$$\pm \frac{RV_o}{r \sin \alpha} \quad \text{i.e.} \quad \begin{cases} \widetilde{v_2} \simeq \dfrac{RV_o}{r \sin \alpha} \\[4mm] v_1 \simeq -\dfrac{RV_o}{r \sin \alpha} \end{cases} \tag{20}$$

From (18) we see that the average velocity is $\simeq \vec{V}_o$, as it should be. From (15) we get for the density:

$$\frac{n}{n_o} = 1 - \frac{2}{\pi^{1/2}} \int_0^{\frac{V_o}{v_{th}} \frac{R}{r \sin \alpha}} e^{-x^2} \, dx = 1 - \text{erf} \left(\frac{V_o}{v_{th}} \frac{R}{r \sin \alpha} \right) \qquad (21)$$

We can again expand (21) and obtain, for values of $r \gg V_o R / v_{th} \sin \alpha$:

$$\frac{n}{n_o} = 1 - \frac{2}{\pi^{1/2}} \frac{V_o}{v_{th}} \frac{R}{r \sin \alpha} \qquad (22)$$

so that the wake of the moon dies as R/r and is proportional to the ratio of the solar wind velocity and the thermal velocity of the ions along the magnetic field lines. As mentioned earlier, the case $\alpha = 0$ is a special one in which this treatment breaks down.

The solar wind parameters in (21) are V_o, $T_{||}$, and α. We can take into account the relation between α and V_o, given by the consideration that the streamlines in the solar wind have to coincide with the magnetic field lines, in a frame corotating with the sun:

$$\tan = \frac{V_\phi}{V_o} \quad \text{or} \quad \sin \alpha = \frac{V_\phi}{(V_o^2 + V_\phi^2)^{1/2}} \qquad (23)$$

Since the azimuthal velocity of the solar wind at 1 a.u. amounts only to a few km/sec, (Weber and Davis, 1967; Modisette, 1967; Alfonso-Faus, 1968), we can take V_ϕ as the angular rotation velocity of the sun times one a.u., i.e. about 430 km/sec. Thus, equation (21) can be expressed in terms of $T_{||}$ and V_o alone, by means of (16) and (23):

$$\frac{n}{n_o} = 1 - \text{erf} \ [(\frac{MV^2_o}{2kT_{||}})^{1/2} \ \frac{(V^2_o + V^2_\phi)^{1/2}}{V_\phi} \ \frac{R}{r}] \tag{24}$$

In Figure 3 we have a plot of the distance r at which $n/n_o = 0.1$ and $n/n_o = 0.5$, in terms of V_o and $T_{||}$, according to (24). Taking $T_{||} = 10^5 \ °K$ and $V_o = 350$ km/sec, we get $n/n_o = 0.1$ at $r \simeq 9$ R and $n/n_o = 0.5$ at $r \simeq 22.5$ R; thus, all the surfaces of constant density ≤ 0.5 are located inside the cold plasma wake and within a distance of 22.5 R from the moon, while the ones with constant density ≤ 0.1 are within a distance of 9 R from the moon. Since the average velocity is $\simeq V_o$, the arguments also apply for the surfaces of constant flux. We will later show that these distances are significantly shortened by electron pressure.

5. Inclination of the Wake

Though we have been referring to the "axis" of the wake, having in mind the cylinder of the cold plasma approach, it is clear that the presence of the magnetic field introduces an asymmetry, except for the particular cases $\alpha = 0°$ and $\alpha = 90°$, so that the curves of constant density will not peak at the "axis" $\lambda = 0$ (Figure 7). We now want to find the line formed by the points at which the curves of constant density peak, i.e. the line defined by the condition:

$$(\frac{dr}{d\lambda}) = 0 \tag{25}$$

$$n = \text{constant}$$

This line gives us a measure of the inclination of the wake. The relation between r and λ is given implicitly by (15), with n = constant, where the limits of integration are functions of r and λ given in (14).

Thus, differentiating (15) with respect to λ we get the equation for $dr/d\lambda$:

$$\frac{\partial}{\partial\lambda} \int_{v_1}^{v_2} e^{-(v_\| /v_{th})^2} \, dv + \frac{dr}{d\lambda}\frac{\partial}{\partial r} \int_{v_1}^{v_2} e^{-(v_\| /v_{th})^2} \, dv_\| = 0 \tag{26}$$

and taking into account (25) we get the equation for the so-defined axis:

$$\frac{\dfrac{\partial v_2}{\partial\lambda}}{\dfrac{\partial v_1}{\partial\lambda}} = e^{\;(v_2^2 - v_1^2)/v_{th}^2} \tag{27}$$

so that using (14) and expanding in terms of R/r we get the approximation to (27)

$$1 + \frac{4\,R}{r\tan\alpha} + 0\,[\frac{R}{r}]^2 = \exp\,(\frac{4\lambda R V_o^2}{r^2\sin^2\alpha\,v_{th}^2} + 0\,[\frac{R}{r}]^3\,) \tag{28}$$

If the exponent in (28) is much less than 1 in absolute value, i.e. if

$$r^2 \gg \frac{4\,|\lambda|\,R}{\sin^2\alpha} \frac{V_o^2}{v_{th}^2} \tag{29}$$

then we can expand the exponential and obtain:

$$\lambda \simeq -r \; \frac{\sin 2\alpha}{2} \; \frac{v^2_{th}}{v^2_o} \tag{30}$$

Expression (30) is the desired equation for the axis of the wake.
It is seen that it is a second order effect in the ratio of the thermal
to the solar wind velocities; for $\alpha = 0$ we get a symmetric wake,
$\lambda = 0$, as expected; the maximum inclination occurs for $\alpha = 45°$ which
is very close to the actual value in the solar wind at 1 a.u.

The range of values of r, for which (30) is a valid expression,
is given by condition (29). Substituting (30) into (29) we get for this
range:

$$r \gg \frac{4 R}{\tan \alpha}$$

One gets the usual breakdown for $\alpha = 0$. In the case of the moon, $\tan \alpha$
is of order 1 and therefore (30) is a good approximation for $r \gg 4R$.
The negative sign in (30) means that the wake is inclined toward
the magnetic field lines; this small effect is given by the angle:

$$\beta \simeq \frac{\sin 2\alpha}{2} \; \frac{v^2_{th}}{v_o^2}$$

Taking $T_{||} = 10^5 \; °K$ and $V_o = 350$ km/sec we get $\beta = .4$ degrees.

We have found the equation for the axis of the wake based upon the
family of curves of constant density. We can do a similar treatment
based upon the family of curves of constant flux parallel to $\vec{V}_o$. The
result is:

$$\lambda \simeq -\frac{3}{2} \; r \frac{\sin 2\alpha}{2} \; \frac{v^2_{th}}{V_o^2} \tag{31}$$

Comparing (31) with (30) we see that the line of peaks of constant
fluxes is inclined 50% more than the line of peaks of constant density.

6. Results and Comparison with Experiments

In Figure 4 one has the orbit of Explorer 35 as it crosses the boundaries of the wake. The plasma flow is observed to decrease from the original interplanetary conditions between a and b; between b and c only instrumental noise was recorded and between c and d the plasma flow is observed to increase toward the interplanetary conditions. We see that the gross features of the structure of the wake, obtained from the treatment of the ion component alone, are in agreement with the observations reported by Lyon et al., 1967. The additional effects produced by electron pressure, electric and magnetic fields, are important per se since they produce observable effects, as shown in the next sections, but they do not alter the general features predicted by the treatment of the ions alone.

7. Effect of Electron Pressure

The electron pressure bends the ion trajectories toward the interior of the cylinder. The amount of bending is given by the balance between the gradients of electron pressure and the inertia of the ions, i.e. Newton's law:

$$-\sin^2 \alpha \cdot \frac{\partial p}{\partial \lambda} = n_o M \frac{v_o^2}{r_c} \tag{32}$$

where r_c is the radius of curvature of the ion's trajectory. Measuring λ and r_c in units of lunar radii, equation (32) gives the order of magnitude for r_c:

$$\sin^2 \alpha \cdot 2p \approx n_o M \frac{v_o^2}{r_c} \tag{33}$$

and using the equation of state for the electron gas

$$p = n_o k T_e \tag{34}$$

we get the estimate

$$r_c \simeq \frac{M \, V_o^2}{2 \, k \, T_e} \quad \frac{1}{\sin^2 \alpha} \tag{35}$$

In Figure 5 we have the sketch of the trajectory of a typical ion and the relevant geometry to find the distance d_e at which the ion crosses the axis of the wake. From the triangle abc:

$$d_e^2 = r_c^2 - (r_c - 1)^2 = 2 \, r_c - 1$$

and since $r_c \gg 1$, we get

$$d_e \simeq (2 \, r_c)^{1/2} \tag{36}$$

Taking into account (35), one obtains:

$$d_e \simeq (\frac{M \, V_o^2}{k \, T_e})^{1/2} \cdot \frac{1}{\sin \alpha} \tag{37}$$

Let us find an estimate of the length for the case of the ions alone: either from (22) or by considering that a typical ion bordering the cylinder has a velocity $\vec{V}_o$ plus a thermal component $(kT_\parallel/M)^{1/2}$ along the magnetic field lines; the length of the ion wake can be given approximately by the distance d_i covered by the ion in arriving at the axis of the cylinder:

$$d_i \simeq V_o \, t/R$$

$$R = (kT_\parallel/M)^{1/2} (\sin \alpha) \, t$$

and eliminating t from the above expressions:

$$d_i \simeq (\frac{MV_o^2}{kT_\parallel})^{1/2} \quad \frac{1}{\sin \alpha} \tag{38}$$

In Figure 5 we have the geometry of the combined effect. Taking into account that the angles ε_1, ε_2, ε_3 are small, we proceed to calculate them.

The angle ε_1, due to the ion thermal motion, is given by

$$\varepsilon_1 \simeq \frac{1}{d_i} \tag{39}$$

while the angle ε_2, due to the electron pressure, is given by

$$\varepsilon_2 \simeq \frac{d_e}{r_c}$$

or using (36) one gets

$$\varepsilon_2 \simeq \frac{2}{d_e} \tag{40}$$

For the angle 2 ε_3 we obtain

$$2\,\varepsilon_3 \simeq \frac{fb}{r_c} \simeq \frac{d_e - d}{r_c}$$

and using (36) to eliminate r_c

$$\varepsilon_3 \simeq \frac{d_e - d}{d_e^2} = \frac{1}{d_e} - \frac{d}{d_e^2} \tag{41}$$

where d is the length due to the combined effect.

The distance ef can be expressed in two different ways:

$$ef \simeq af\;\varepsilon_1 \simeq fb\,(\varepsilon_2 - \varepsilon_3)$$

and substituting af, fb from Figure 5, and using (39), (40) and (41) we get

$$\frac{d}{d_i} \simeq (d_e - d)\,(\frac{1}{d_e} + \frac{d}{d_e^2}) = 1 - \frac{d^2}{d_e^2}$$

The above equation gives for d, using (37) and (38)

$$d = (\frac{MV_o^2}{kT_{\parallel}})^{1/2} \ \frac{1}{\sin \alpha} \ \frac{1}{2} \frac{T_{\parallel}}{T_e} \ [(1 + 4 \frac{T_e}{T_{\parallel}})^{1/2} - 1] \qquad (42)$$

As a check, the above expression gives $d \to d_i$ when $T_e \to 0$ and $d \to d_e$ when $T_{\parallel} \to 0$, as it should be.

Now we can define an effective temperature to take into account the effect of two electrons on the length of the wake. Identifying (42) to

$$(\frac{MV_o^2}{kT_{eff}})^{1/2} \ \frac{1}{\sin \alpha}$$

one obtains

$$\frac{T_{eff}}{T_{\parallel}} = \frac{1}{2} \ [1 + 2 \frac{T_e}{T_{\parallel}} + (1 + 4 \frac{T_e}{T_{\parallel}})^{1/2}] \qquad (43)$$

Hence, a better approximation to the distribution of densities and fluxes is immediately obtained by considering the ions to be alone, as done in the corresponding section, with the effective temperature T_{eff} defined in (43). Table I presents characteristic numerical values for the effective temperature. If $T_e/T_{\parallel} = 2$ then the length of the wake is shortened by a factor of 2 due to electron pressure.

TABLE I

Effective Temperature of the Ions in Terms of Electron Temperature

$\dfrac{T_e}{T_{\parallel}}$	$\dfrac{T_{eff}}{T_{\parallel}}$
1	2.62
2	4.00
3	5.30
4	6.56

8. Electric Fields

In order to get the effect of the electrons upon the ions at short distances from the moon, one has to analyze in detail the structure of the interaction, i.e. charge separation and electric fields rather than bulk pressure; thus, the problem now is to solve Poisson's equation for the two component plasma. Consider the electrons to be in thermal equilibrium, with a Maxwellian distribution function modified by the Boltzmann's factor due to the presence of an electric potential ϕ. The density of electrons is given by

$$n_e = n_o \exp (e\phi / kT_e) \tag{44}$$

Using $R_\mathbb{C}$ as the unit of distance, and calling

$$\Phi = - e\phi/kT_e \tag{45}$$

the electric potential satisfies

$$\nabla^2 \Phi = (\frac{R}{D})^2 \ [\ n_i/n_o - \exp (- \Phi)] \tag{46}$$

where D is the Debye length $(kT_e/4\pi n_o e^2)^{1/2}$. Since $D << R_\mathbb{C}$, it is convenient to express the solution of (46) in a power series expansion in terms of $(D/R_\mathbb{C})^2$. The zero order solution is:

$$\Phi \simeq \ln \frac{n_o}{n_i} \tag{47}$$

and the expansion is valid if

$$\frac{n_o}{n_i} \ (\frac{D}{R})^2 \ \nabla^2 \ [\ \ln \frac{n_o}{n_i} \ ] \ << 1 \tag{48}$$

It is seen that the electrons dominate the central part of the wake, since the curvature of the potential has to change sign in order to match the other boundary, according to Figure 6.

The line termed "limit of $n_i \simeq n_e$" corresponds to the breakdown

of the condition (48) for the validity of the solution $\Phi \simeq \ln (n_o/n_i)$.

After a distance of $\simeq 2.7$ radii from the moon, the condition (48) is

satisfied for all values of λ, which means that almost no charge separation

occurs, as usual in a plasma. At distances shorter than 2.7 radii charge

separation occurs only at points well inside the wake, where the density

is extremely small. The line termed "limit of plasma state" has been

drawn by looking for the locus of points at which there is only one

particle per Debye sphere. At short distances, from the back of the

moon, the gradients of the potential are mainly perpendicular to the

axis of the wake, which means that we can express the electric fields as:

$$E \simeq \frac{\partial \Phi}{\partial \lambda} \tag{49}$$

in units of kT_e/R. From Figure 6 it is seen that the slope (49)

increases rapidly as the ion penetrates the wake; a typical ion that

enters the wake with the velocity of the bulk plasma $\vec{V}_o$, and a thermal

component v_i parallel to the magnetic field lines, is falling into a

potential of some kT_e/e units, which means that its velocity normal

to the wake increases by a factor of some units. Since the effect is

important in determining the width of the boundary, we want to find

the ion trajectories in the presence of the electric potential.

First, let us find an approximate analytical expression for

the density of the ions, in the absence of the potential: the time for

an ion to arrive at a distance r from the moon is $t \simeq r/V_o$; hence,

the thermal component along the magnetic field lines that is necessary

for the ion to penetrate a distance $1 - \lambda$ into the wake, is given by

$$v \simeq \frac{1 - \lambda}{t \sin \alpha} \simeq \frac{1 - \lambda}{r \sin \alpha} \ V_o \tag{50}$$

Since the number of ions in the state (50) is proportional to the Boltzmann's factor, we get finally:

$$n = \frac{n_o}{2} \, \exp \left[-\left(\frac{V_o}{v_i \, \sin \alpha} \right)^2 \, \left(\frac{1-\lambda}{r} \right)^2 \right] \tag{51}$$

Expression (51) is an approximation to the density curves of Figure 6. It is seen that the constant density curves are given by straight lines. From (47), (49) and (57) we get for the electric field

$$E \simeq -2 \, \frac{M}{e} \, \frac{V_o^2}{R} \, \frac{T_e}{T_{||}} \, \frac{1}{\sin^2 \alpha} \, \frac{1-\lambda}{r^2} \tag{52}$$

We consider the initial conditions along the line $\lambda = 1$, i.e. the boundary of the wake in the cold-plasma approximation; along this line, a typical ion has a bulk velocity $\vec{V}_o$, plus a thermal component v_i along the magnetic field lines. The initial conditions are therefore:

$$t = 0, \; r = r_o, \; \lambda = 1, \; \frac{d\lambda}{dt} = -\frac{v_i \, \sin \alpha}{R} \tag{53}$$

where r_o is the initial position on the line $\lambda = 1$. Since $V_o \gg v_i$, the motion of the ion projected along the $\vec{V}_o$ direction is a uniform one. Along the direction perpendicular to $\vec{V}_o$ the ion is accelerated by the electric field (52). Thus, the equations of motion are:

$$r = r_o + \frac{V_o t}{R}$$

$$\frac{d^2\lambda}{dt^2} = -2 \, \frac{V_o^2}{R} \, \frac{T_e}{T_{||}} \, \frac{1}{\sin^2 \alpha} \, \frac{1-\lambda}{r^2} \tag{54}$$

To integrate the system (54) we differentiate the first equation:

$$dr = V_o/R \; dt \tag{55}$$

and substituting (55) into the second one we get:

$$\frac{d^2\lambda}{dr^2} = -2 \frac{T_e}{T_{\|}} \frac{1}{\sin^2 \alpha} \frac{1 - \lambda}{r^2}$$

i.e. a second order linear differential equation with variable coeffieients. The solution gives the trajectory of the ion:

$$\lambda = \frac{v_i \sin \alpha}{v_o} \frac{1}{2m-1} r \left\{ \frac{r_o}{r})^m - (\frac{r}{r_o})^{m-1} \right\} + 1 \tag{56}$$

where

$$m = \frac{1}{2} + (\frac{1}{4} + 2 \frac{T_e}{T_{\|}} \frac{1}{\sin^2 \alpha})^{1/2} \tag{57}$$

In order to find the new density, consider two trajectories separated by a small distance dr_o along the line $\lambda = 1$. The separation along a general line $\lambda = $ constant will be given by dr. The relation between dr_o and dr is found by differentiating (56), considering $\lambda = $ constant. Under steady state conditions, the flux of ions normal to the element dr_o must be equal to the flux normal to dr:

$$1/2 \, n_o v_i \sin \alpha \, dr_o = n \, |v_\lambda| \, dr \tag{58}$$

where v_λ is the component of the velocity of the ion along the λ axis. It is obtained by differentiating (63).

From (58) we get

$$n = \frac{n_o}{2} \, [(m-1) \, (\frac{r}{r_o})^m + m(\frac{r_o}{r})^{m-1} \,]^{-1} \, (2m-1) \tag{59}$$

where r and r_o are linked by the equation of the trajectory (56). The density is therefore given by the system (59) and (56), where r_o is just a parameter to be eliminated between the two equations of the system.

From (59) it is seen that the curves of constant density are given
by values of r/r_0 = constant and substituting this constant into (56)
one finds that the curves of constant density are straight lines, as
in the previous case given in (51), except that now the equation is

$$\frac{1 - \lambda}{r} = \frac{v_i \sin \alpha}{V_0} \quad \frac{1}{2m-1} \quad [(\frac{r}{r_0})^{m-1} - (\frac{r_0}{r})^m] \tag{60}$$

where r/r_0 is given by (59) for a particular value of the density.
It is seen that the effect of the electrons is to modify the inclination
of the lines of constant density. In the case of no electron pressure
(57), the inclination of these lines is proportional to:

$$[\ln (\frac{n_0}{2n})]^{1/2} \tag{61}$$

while in the present case (60) it is proportional to:

$$\frac{1}{2m-1} \quad [(\frac{r}{r_0})^{m-1} - (\frac{r_0}{r})^m] \tag{62}$$

Since $r/r_0 > 1$ and $m > 1$, we can see that there are two different effects
due to electron pressure: for small values of the density, the dominant
terms in (59) and (60) are the first exponentials; this implies that
if T_e increases, m increases, and the constant density lines become
more inclined; for values of the density close to the unperturbed
conditions, the first exponentials in (59) and (60) are of order unity,
which implies that the dominant term in (62) is the factor $1/(2m-1)$;
thus, if T_e increases, this factor decreases and the constant density
lines become less inclined. This imposes that there must be a neutral
line of intermediate density that remains unaltered by the electron
pressure. This line is obtained by equating (61) and (62). Thus,
above the neutral line the density decreases and below it, i.e. at the
inner part of the wake, the density increases; this is the smoothing

effect of the electron pressure since it weakens the gradients of density across the boundary.

9.   Surface Currents and Magnetic Field Distortion

In this final section we analyze the distortion of the magnetic field, due to the presence of surface currents at the boundary of the wake. This effect arises because of the circling motion of the particles around the magnetic field lines, and the sudden drop in density across the boundary of the wake. Since the ions and electrons circle the magnetic field lines in opposite senses, both components add up to the final current. Recent measurements (Hundhausen et al., 1967) indicate that $T_{\perp}$ for the ions is about a factor of 5 or 10 times smaller than the electron temperature; hence, the effect is mainly due to the electron thermal motions.

We interpret the mechanism as follows: the ions carry most of the inertia of the solar wind, and near the back of the moon they give rise to an empty cylinder, as presented in the cold-plasma approach. The effect of the thermal motions of the ions and electrons does not modify this picture in any drastic way; the thermal motions make the drop of density more or less steep across the boundary, though they are important in determining the length of the wake. Here we are interested in analyzing the region close to the back of the moon, where the drop in density is sharpest, and we will consider the idealized situation where the drop occurs within a Larmor distance. Once the magnetic field is distorted, there will be additional effects coming from the currents that appear because of the drifts, due to the gradients of the field and its curvature. Nevertheless, we consider that the drop in density is the primary source for the distortion in the magnetic field.

Consider the case of the magnetic field lines parallel to the solar wind velocity; the circling particles will have part of their trajectory inside the cylindrical cavity and, since the penetration is of the order of the Larmor's distance which is much smaller than the radius of the moon, we can consider the resultant currents as a system of surface currents. The situation is similar to the mechanism of a solenoid.

An estimate of the current per unit length is obtained in the following way: the density in the transition zone is $\approx n_o/2$, since all the particles in this region come from the exterior of the cylinder, and none from the interior. Considering an element of surface in this region, parallel to the magnetic field lines, each particle crosses it $\omega_e/2\pi$ times per second, where ω_e is the electron cyclotron frequency. The penetration of the particles into the cylinder is proportional to the area πL_e^2, oriented in the plane normal to the cylinder, where L_e is the Larmor radius. Hence, the current per unit length is given by:

$$I_\ell \simeq \frac{n_o}{2} \; \frac{\omega_e \cdot e}{2\pi} \; \pi \; L_e^2 \tag{63}$$

Considering typical electrons, we may use the relations $\omega_e \, L_e = v_{the \perp}$, $\omega_e = e \, B_o/mc$ and $1/2 \, mv^2_{the \perp} = kT_e$ so that (63) gives

$$I_\ell \simeq \frac{1}{2} \; \frac{n_o kT_e}{B_o} \; c \tag{64}$$

We are interested in the functional dependence of the magnetic distortion on the solar-wind parameters, at the central part of the wake. Thus, we will take I_ℓ as given by (64) times a constant f that may be determined experimentally by fitting a particular observation:

$$I_\ell = f \frac{1}{2} \frac{n_o kT_e}{B_o} c \qquad (65)$$

In Figure 7 we have the situation for a general magnetic field inclination α. The currents are contained in parallel planes oriented perpendicularly to the magnetic field lines, so that they are tangential to an ellipse. We project the currents along the direction of the axis of the wake, $I_{||}$, and on the plane normal to the axis, $I_\perp$:

$$I_{||} = I_\ell \sin^2 \alpha \; \frac{\cos^2 \psi}{(1 - \sin^2\alpha \; \sin^2\psi)^{1/2}} \; d\psi \qquad (66)$$

$$I_\perp = I_\ell \cos^2 \alpha \; \frac{1}{(1 - \sin^2\alpha \; \sin^2\psi)^{1/2}} \; dr \qquad (67)$$

Now we apply the Biot and Savart law:

$$\vec{B} = \frac{1}{c} \int I \frac{\vec{d\ell} \times \vec{h}}{h^3} \qquad (68)$$

to the two systems of currents (66) and (67). Starting with $I_\perp$, from the ψ dependence it is seen that this current gives a magnetic field contribution only along the r axis:

$$dB_r = \frac{1}{c} \int I_\perp \frac{d\psi}{h^3}$$

$$= \frac{4}{c} I_\ell \; \cos^2\alpha \frac{1}{h^3} \cdot K(\sin \alpha) \; dr$$

where $K(\sin \alpha)$ is the complete elliptic integral of the first kind. Now, instead of integrating with respect to r, we integrate with respect to β

and obtain:

$$B_r = \frac{4}{c} \, I_\ell \, \cos^2\alpha \, \, K(\sin \alpha) \, \, (\cos \beta_1 + \cos \beta_2) \tag{69}$$

where β_1 and β_2 are defined in Figure 8. Here we do not worry about the final sign, since we know that the distortion is such that both components of the undisturbed magnetic field are increased inside the wake, due to the absence of the magnetic moment of the plasma particles.

The contribution from $I_{||}$ is found by applying (68) with $\vec{d\ell}$ parallel to the r axis (Figure 8). From the ψ dependence it is seen that the contribution of this component gives a magnetic field along the $-\lambda$ direction. Again, we first integrate with respect to the β variable, instead of r, and then integrate with respect to ψ to obtain:

$$B_\lambda = \frac{4}{c} \, I_\ell \, \sin^2 \alpha (\cos \beta_1 + \cos \beta_2) \, \left(\frac{\alpha}{\sin \alpha} + \frac{\cos \alpha}{2 \sin^2\alpha} \right.$$

$$\left. - \frac{\alpha}{2 \sin^3\alpha} \right) \tag{70}$$

In the above expression, the value $\alpha = 0$ gives $B_\lambda = 0$, as it should.

The total increase in the magnitude of the magnetic field is given by:

$$\Delta B \simeq B_r \cos \alpha + B_\lambda \sin \alpha$$

and from (69), (70) and (65) one obtains:

$$\Delta B \simeq 2f \, (\cos \beta_1 + \cos \beta_2) \, \frac{n_o kT_e}{B_o} \, \, F(\alpha) \tag{71}$$

where

$$F(\alpha) = \cos^3\alpha \, \, K(\sin \alpha) + \alpha \, \sin^2\alpha + 1/2 \sin \alpha \, \cos \alpha - \frac{\alpha}{2} \tag{72}$$

gives the α dependence. From Table II it is seen that $F(\alpha)$ does not vary much with α; for α between 40 and 70 degrees, which are typical

values at 1 a.u., we can take $F(\alpha) \simeq .5$ and get from (71):

$$\Delta B \simeq f \frac{n_o kT_e}{B_o} \quad (\cos \beta_1 + \cos \beta_2) \tag{73}$$

where f is of order unity. Since Explorer 35 orbits at about 2 radii from the back of the moon, we have $\cos \beta_1 + \cos \beta_2 \simeq 1.9$, and using $n_o \simeq 10$, $B_o \simeq 5$ gamma and $T_e \simeq 2 \ 10^{5} {}^{\circ}K$, one obtains

$$\Delta B \simeq 1.05 \ f \ \text{gamma}$$

The above result agrees with the observation from Explorer 35, as presented by Colburn et al., 1967, for a value of f = 1.5. We have arrived at this figure following a different approach than Colburn et al. (1967); these authors consider the equation of motion of the boundary of the cavity, assuming that the drop in plasma pressure is balanced by the increase in magnetic pressure; we believe that this treatment does not apply to this case, according to the following argument: the physical reason for a cavity at the back of the moon is the inertia of the ions, i.e. the fact that their bulk velocity is much higher than their thermal velocity, as seen in the corresponding section of this work. At the boundary, any gradient of pressure will try to modify the inertia of the ions, and the equilibrium should be a dynamical one, not a static one. The surface currents are what they turn out to be because of the interaction of the solar wind with the moon, but they do not play an important role in the formation of the cavity. Their effect on the magnetic field inside the wake is to increase it by an amount given by (73); furthermore, since the "solenoid" is of finite length, the magnetic field outside the cavity, due to the

surface currents, should have an opposite sign compared with the magnetic field inside it; hence, one expects a decrease in the field just outside the boundary, as reported by Colburn et al.,(1967).

Recently Ness et al., (1968) have presented the results from an approximate numerical computation by Whang (1968) valid in the plane of symmetry only, and including the drift currents due to the curvature and gradient of the magnetic field. They express the feeling that these currents produce a small effect compared with the magnetization currents, which agrees with the approach we have taken here. Hence, it is not surprising that our results agree, for the inner part of the wake. For the external part, the theoretical results of Whang (1968) are not in agreement with the observations. Ness et al., (1968) suggest that perhaps higher order iterations are the answer to the problem. An alternative point of view is to postulate the existence of a weak intrinsic magnetic field in the moon, strongly distorted by the solar wind that would project the external parts of the field toward the boundary of the cavity. Future measurements of the magnetic field at the surface of the moon will hopefully close the subject.

TABLE II

Influence of the Inclination of the Field

Upon the Magnetic Distortion

α in degrees	$F(\alpha)$
0	1.571
10	.815
20	.761
30	.657
40	.554
50	.489
60	.415
70	.550
80	.667
90	.785

References

Alfonso-Faus, A., Rotation of the Solar Wind Plasma, Planet. Space Sci. 16, 1-6, 1968.

Colburn, D. S., Currie, R. G., Mihalov, J. D., and Sonett, C. P., Diamagnetic Solar-Wind Cavity Discovered Behind Moon, Science 158, 1040-1042, 1967.

Gold, T., The Magnetosphere of the Moon, in The Solar Wind, Edited by R. J. Mackin and M. Neugebauer, 381-391, Jet Propulsion Laboratory, California, 1966.

Hundhausen, A. J., and Bame, S. J., Solar Wind Thermal Anisotropies: Vela 3 and IMP 3, J. Geophys. Res. 72, 5265-5274, 1967.

Lyon, E. F., Bridge, H. S., and Binsack, J. H., Explorer 35 Plasma Measurements in the Vicinity of the Moon, J. Geophys. Res. 72, 6113-6117, 1967.

Michel, F. C., Shock Wave Trailing the Moon, J. Geophys. Res. 72, 5508-5509, 1967.

Michel, F. C., Magnetic Field Structure Behind the Moon, J. Geophys. Res. 73, 1533-1542, 1968.

Modisette, J. L., Solar Wind Induced Torque on The Sun, J. Geophys. Res. 72, 1521-1526, 1967.

Ness, N. F., Behannon, K. W., Scearce, C. S., and Cantarano, S. C., Early Results from the Magnetic Field Experiment on Lunar Explorer 35, J. Geophys. Res. 72, 5769-5778, 1967.

Ness, N. F., Behannon, K. W., Taylor, H. E., and Whang, Y. C., Perturbations of the Interplanetary Magnetic-Field by the Lunar Wake, Goddard Space Flight Center Preprint X-612-68-12, 1968.

Sonett, C. P., Colburn, D. S., and Currie, R. G., The Intrinsic Magnetic Field of the Moon, J. Geophys. Res. 72, 5503-5507, 1967.

Weber, E. J., and Davis, L., The Angular Momentum of the Solar Wind, Astrophys. J. 148, 217-227, 1967.

Whang, Y. C., Interaction of the Magnetized Solar Wind with the Moon, Goddard Space Flight Center Preprint X-612-67-580, 1967.

Whang, Y. C., Theoretical Study of the Magnetic Field in the Lunar Wake, Goddard Space Flight Center Preprint X-612-68-17, 1968.

Figure Captions

Fig. 1.   Velocity components of an ion.

Fig. 2.   Relative position of the cuts in the Maxwellian distribution
                 function for the ions.

Fig. 3.   Length of the curves of constant density 0.1 and 0.5 in
                 terms of V_O and $T_{\shortparallel}$. The numerical values of $T_{\shortparallel}$ are high
                 in order to allow for the effective temperature defined
                 in the text.

Fig. 4.   Orbit of Explorer 35.

Fig. 5.   Typical trajectories of a "hot" ion with and without electron
                 pressure.

Fig. 6.   Electric potential in the wake.

Fig. 7.   Projection of the system of currents into a circular and
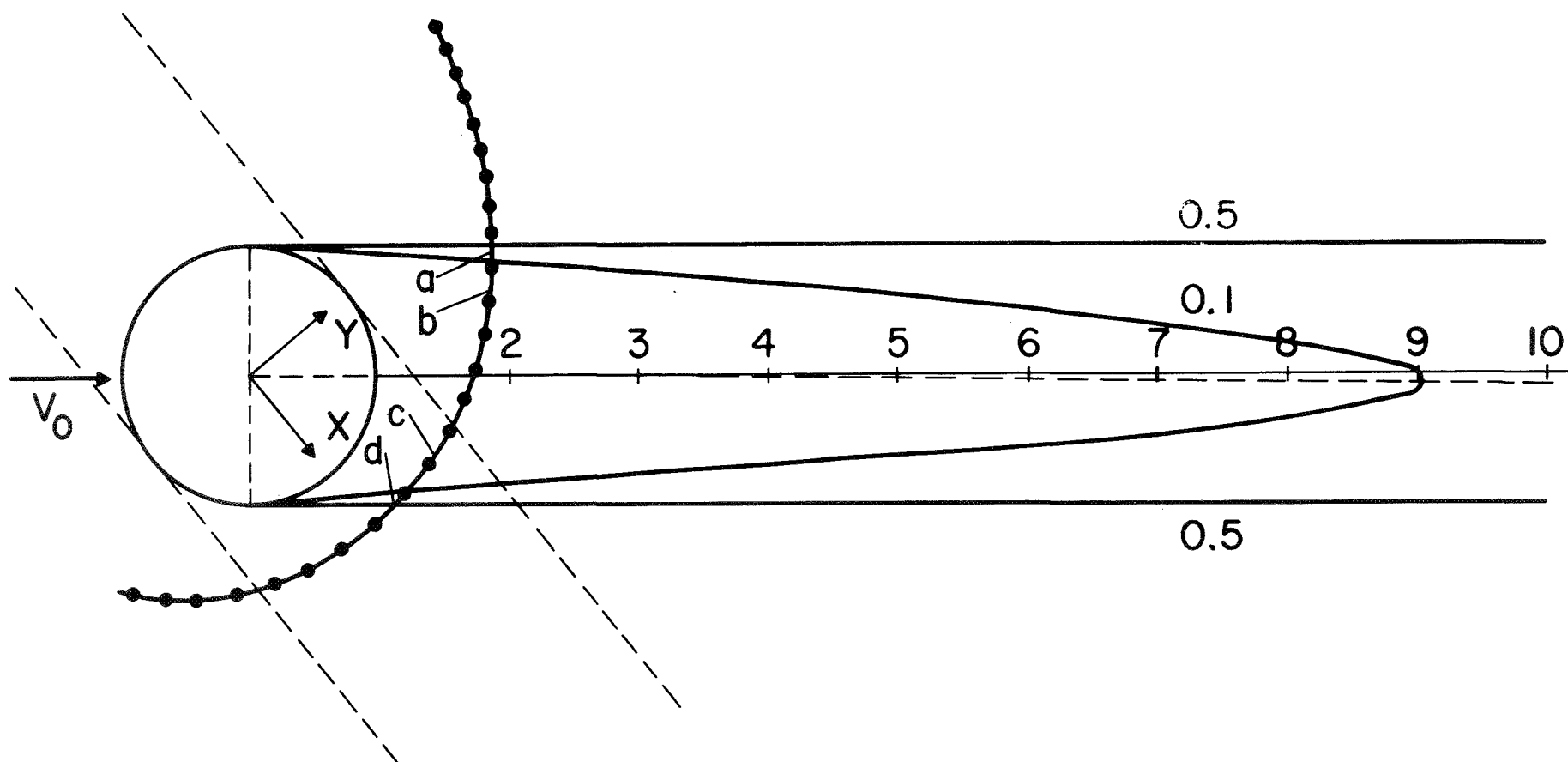   an axial system.

Fig. 8.   Circular and axial system of currents.
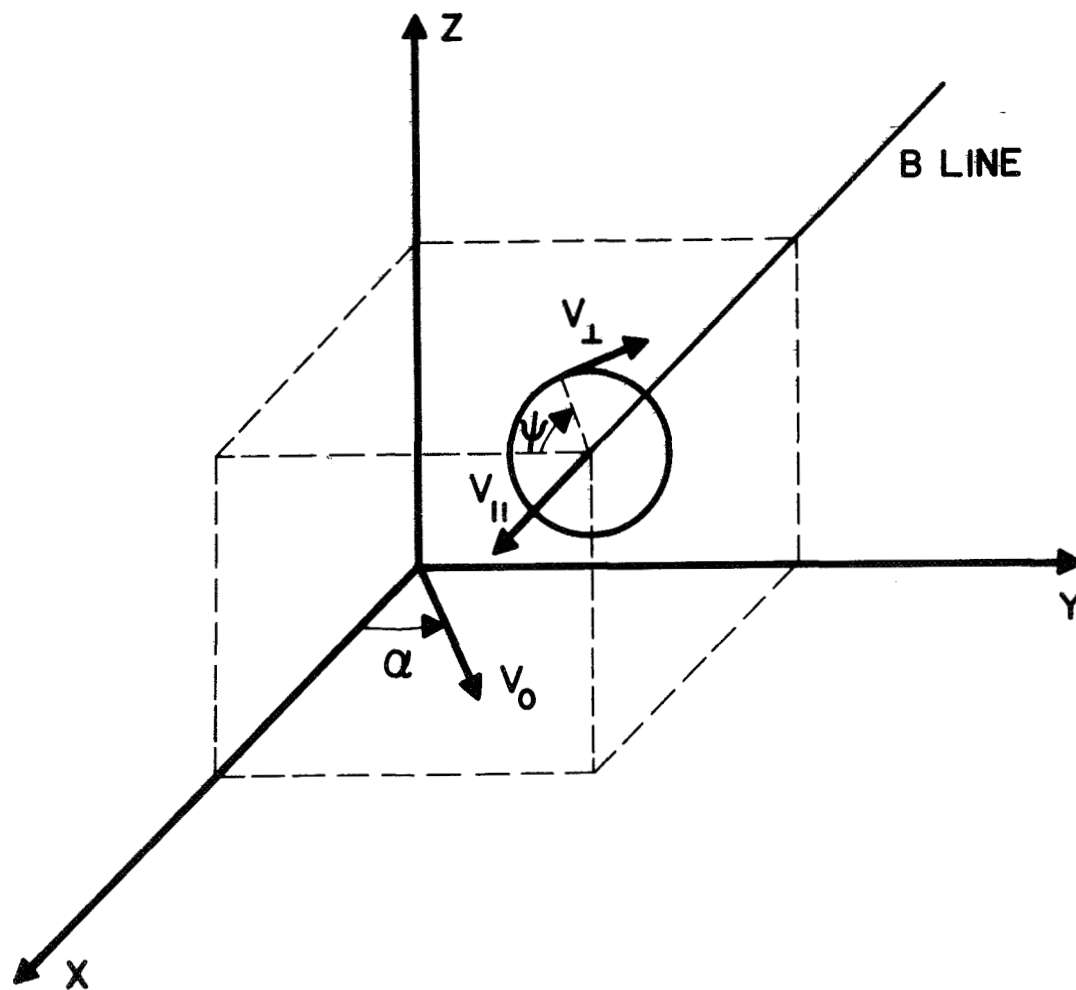
Figure 1
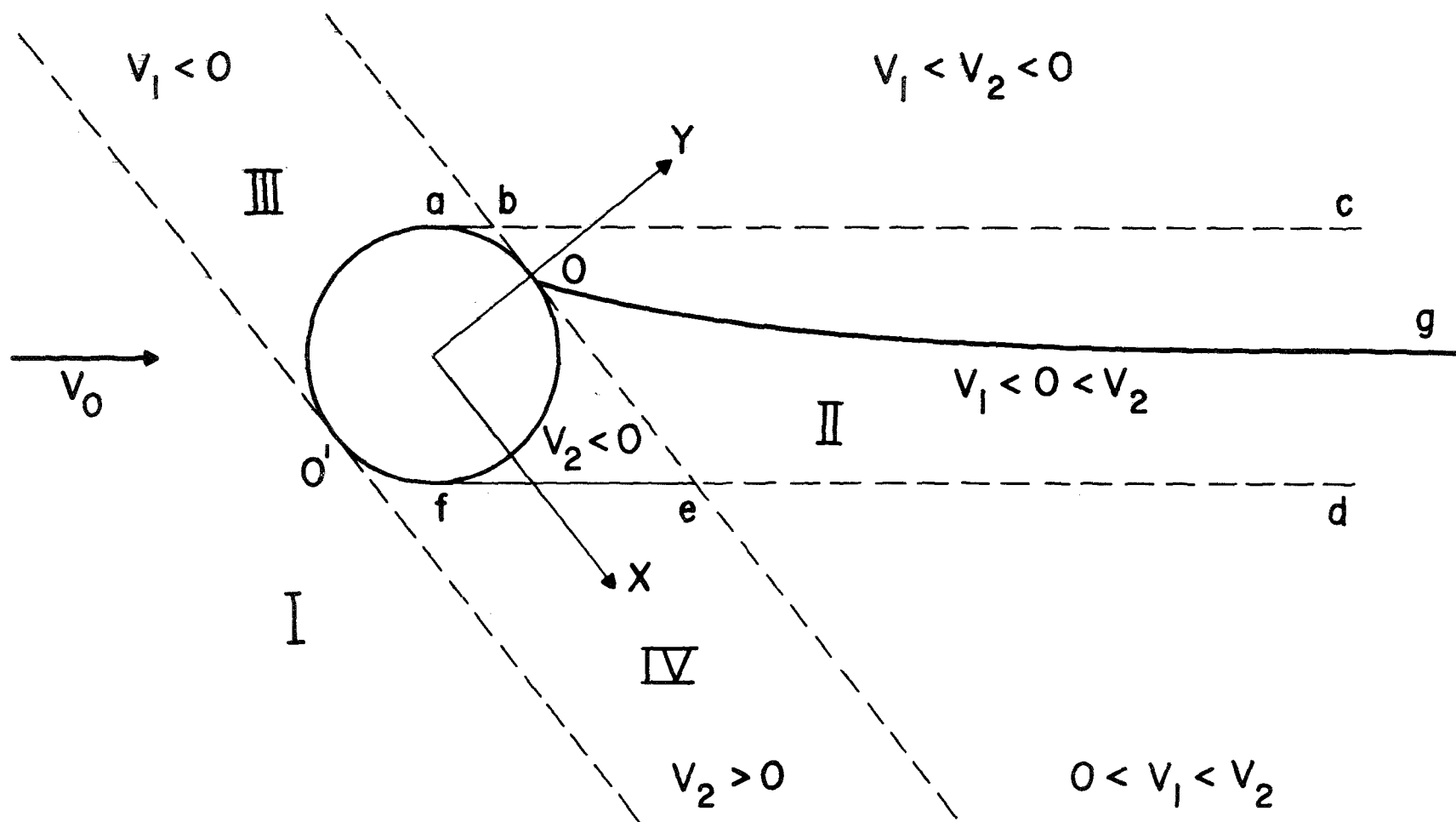
Figure 2

Figure 3

Figure 4

$$ab = d_e$$
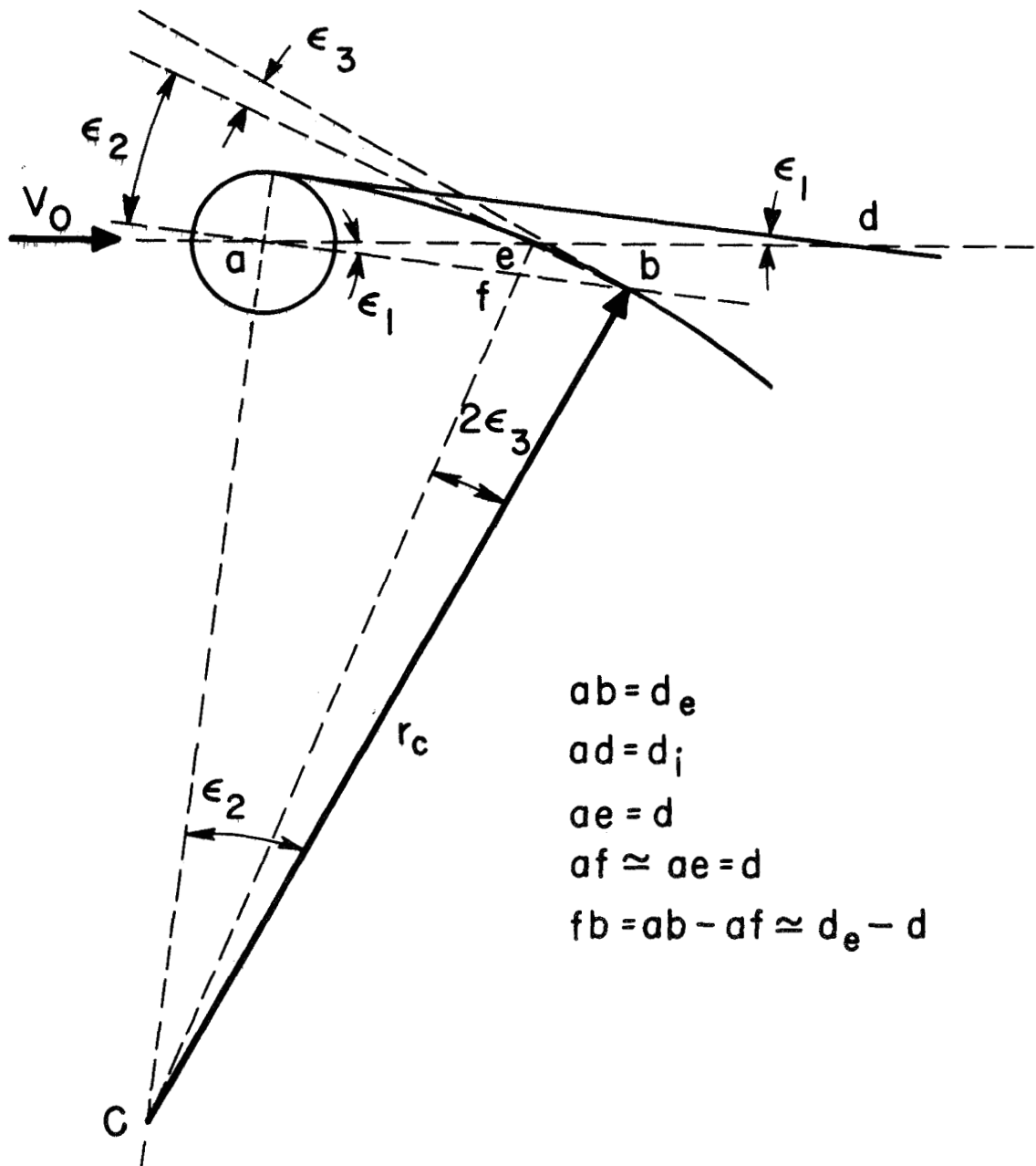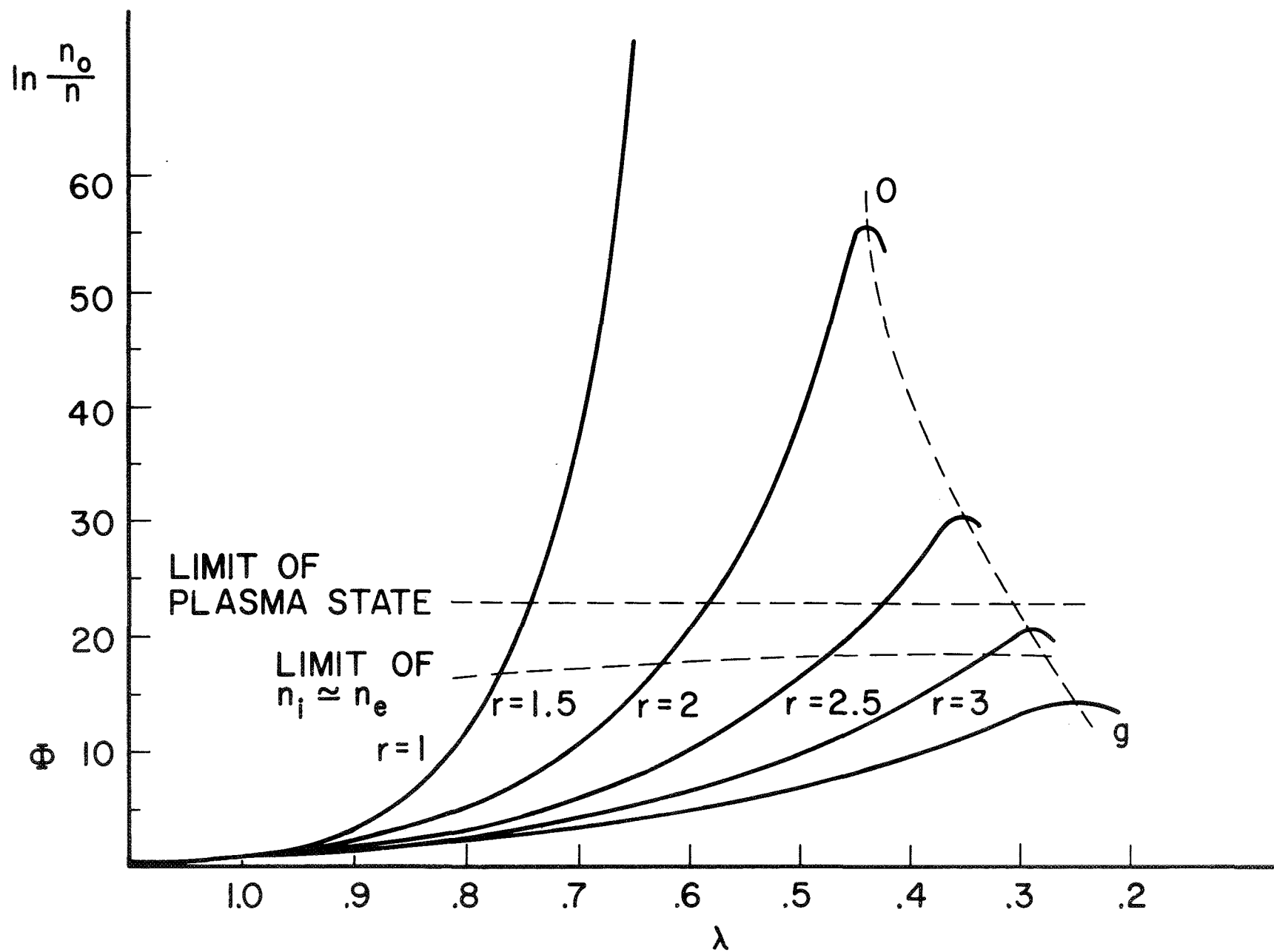$$ad = d_i$$
$$ae = d$$
$$af \simeq ae = d$$
$$fb = ab - af \simeq d_e - d$$
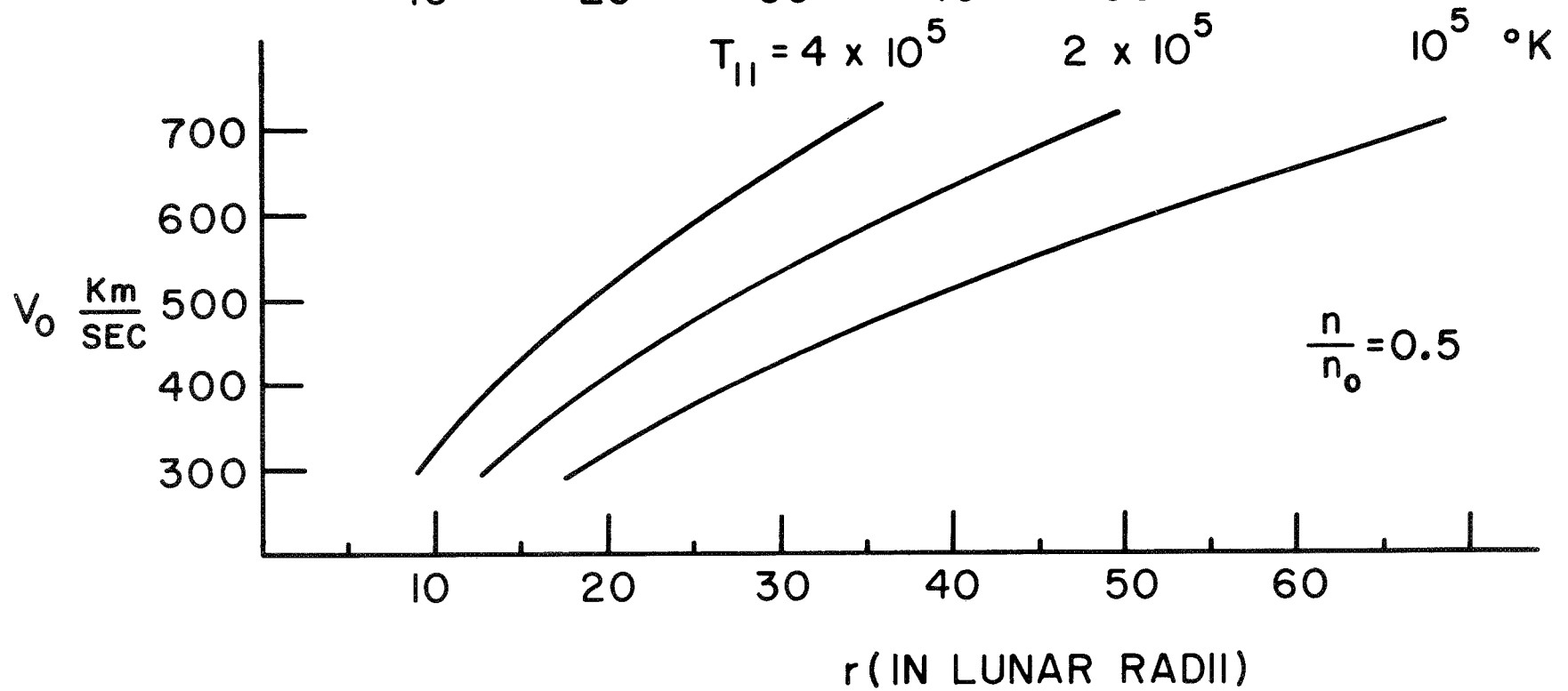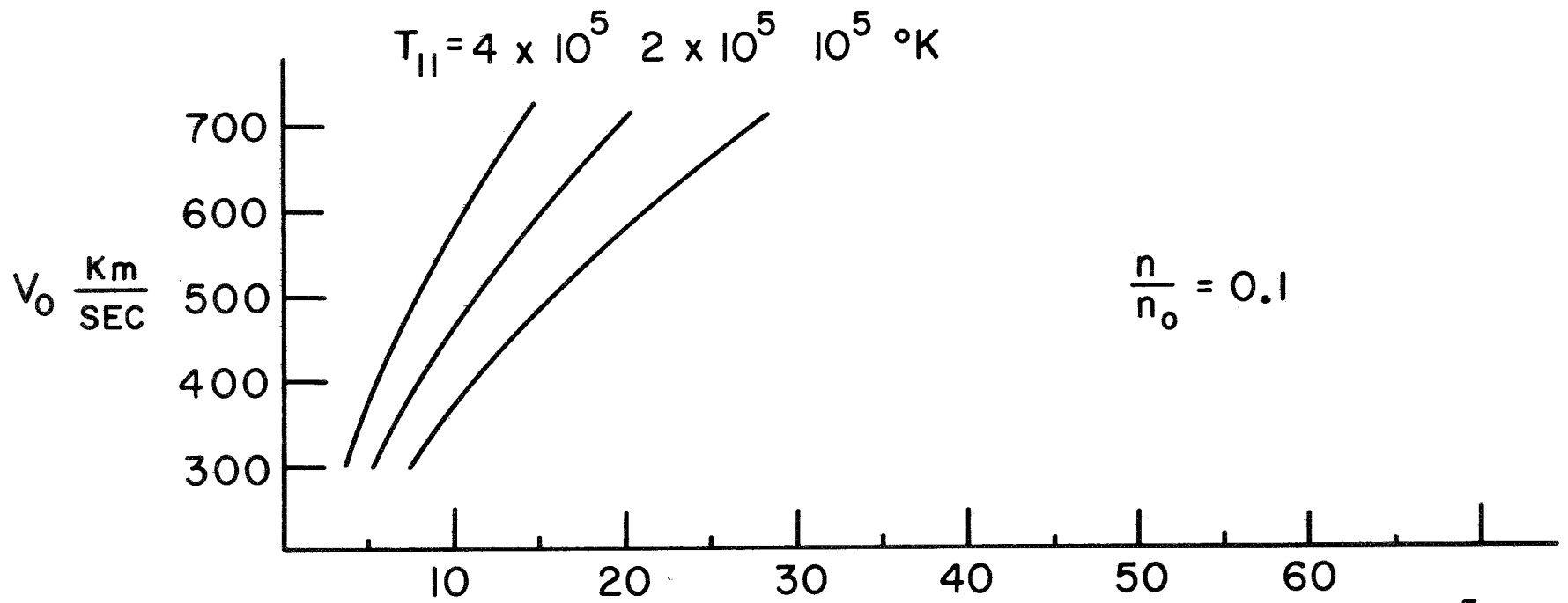
Figure 5

Figure 6

Figure 7

Figure 8